

# We are IntechOpen, the world's leading publisher of Open Access books Built by scientists, for scientists

6,300

Open access books available

170,000

International authors and editors

185M

Downloads

Our authors are among the

154

Countries delivered to

TOP 1%

most cited scientists

12.2%

Contributors from top 500 universities



WEB OF SCIENCE™

Selection of our books indexed in the Book Citation Index  
in Web of Science™ Core Collection (BKCI)

Interested in publishing with us?  
Contact [book.department@intechopen.com](mailto:book.department@intechopen.com)

Numbers displayed above are based on latest data collected.  
For more information visit [www.intechopen.com](http://www.intechopen.com)



Chapter

# Antibacterial Strategies: Photodynamic and Photothermal Treatments Based on Carbon-Based Materials

*David Giancarlo García Vélez, Karina Janneri Lagos Álvarez  
and María Paulina Romero Obando*

## Abstract

The problem of bacterial resistance is based on the abuse of antibiotics such as trimethoprim, fluoroquinolones, chloramphenicol, and some carbapenems. For this reason, conventional treatments to treat diseases caused by bacteria have become ineffective. Therefore, developing new therapies with multifunctional materials to combat bacteria is mandatory. In this context, photodynamic treatment (PDT) and photothermal treatment (PTT) have been proposed to combat bacteria. These light-stimulated treatments are minimally invasive and have a low incidence of side effects. In addition, they are simple, fast, and profitable. The antibacterial effect of PDT, PTT, or synchronic PDT/PTT arises from the generation of reactive oxygen species (ROS) and heat caused by a photoactivated specific photosensitizer (PS) and photothermal agents (PTAs), respectively. The effectiveness of photoinduced treatment depends, among other parameters, on the nature and concentration of the PS/PTAs, light dose, and irradiation wavelength. PS/PTAs based on carbon-based materials (CBMs), such as graphene oxide, reduced graphene oxide, carbon dots, and carbon nanotubes as antibacterial agents, will be discussed in this chapter. These CBMs have emerged as excellent antibacterial alternatives due to their excellent physicochemical properties, biocompatibility, low toxicity in the dark, specificity, and excellent response to light. Moreover, several composites and hybrids employing polymers, metal oxides, and metals have been tested to enhance the antibacterial activity of the CBMs.

**Keywords:** photodynamic therapy, photothermal therapy, carbon-based materials, photosensitizers, photothermal agents

## 1. Introduction

Food and water for human consumption, medical equipment, lung walls, upper respiratory tract, and external wounds, that accommodate a small number of bacteria, can generate a potential health risk due to their high adaptability and bacterial proliferation [1]. Infections caused by bacterial pathogens have claimed many human and

animal lives, mainly when the development of antibacterial treatments is deficient, for example, the plague pandemic coined as the “black death” in medieval Europe caused by the bacterium *Yersinia pestis*, cholera (*Vibrio cholera*), and tuberculosis (*Mycobacterium tuberculosis*), among others. Likewise, viral pathogens such as HIV and COVID-19 can suppress the immune system, leading to enhanced conditions for coinfection with bacterial pathogens [2, 3]. The shortage of drinking water and medical procedures exposed to bacterial pathogens in the air, or contaminated medical instruments, have become problems of great interest to the world because they are sources that produce bacterial infections that can lead to the death of people, mainly in developing countries [3, 4]. Bacterial infections significantly affect the health of people with cancer, diabetes, and HIV and transplant patients, a high-risk population. Likewise, they considerably affect the wound healing mechanism, reaching the amputation of affected regions or limbs [5, 6].

Antibiotics emerged in the previous era (1940–1980, the “Golden Age” of antibiotics) as an effective treatment for bacterial infectious diseases caused mainly by *Streptococcus pneumoniae* and *Staphylococcus aureus* [3, 6]. Undoubtedly, the general administration of antibiotics revolutionized the treatment of infections caused by pathogenic bacteria, saving countless lives, and they are still considered of great importance in modern bacterial therapies [1, 6]. Antibiotics are a subgroup of antimicrobial agents classified according to their effect, mechanisms of action, and spectrum. Antibiotics are designed to inhibit the growth and multiplication of susceptible bacterial cells selectively, interfering with the synthesis of the bacterial cell wall, protein synthesis, and nucleic acid synthesis, or affecting metabolic pathways [7, 8]. If antibiotic inhibits cell growth and multiplication, they are bacteriostatic, while when they cause internal mechanisms that lead to cell death, they are known as bactericides. However, they present specific mechanisms of action depending on the type of cell membrane of gram-positive or gram-negative bacteria. Likewise, they are broad spectrum when they can eliminate bacteria of both types [8]. Bacteria show the affinity of forming colonies in any solid or liquid substrate (catheters, prosthetics, human body parts, heart valves, and teeth), and proliferation in the presence of nutrients to release exopolysaccharides gives rise to biofilms [3, 6].

Biofilms are associated with the physiological states of bacteria and can be monostrains or multistrains, and there may be synergy or antagonism between the different strains [9, 10]. These biofilms are extremely difficult to eradicate because of the extracellular matrix (exopolysaccharides) that prevents the diffusion of antibiotics in the structure of the biofilm, as well as prevents the free entry and exit of nutrients and waste from bacteria. This situation leads to metabolic reduction (a subcritical condition that activates bacterial survival mechanisms). Therefore, most antibiotics become deficient because they were designed for exponential growth conditions [4, 6, 11].

Biofilms of multidrug-resistant (MR) bacteria are considered a source of infection that generates a high risk of affecting and causing death to people at any stage of life. For this reason, these biofilms are urgent public health problems in the world, charging 10 million human lives per year and costing 100 billion dollars by 2050 in the world economy. Thus, this strengthens the challenge to innovate current antibacterial treatments since the exchange processes of the genetic expression of bacterial pathogens are linked to the food chain, water sources, clinical care, and the environment in general, modifying the virulence of bacterial pathogens [3, 4, 6, 12], as shown in **Figure 1a**.

Searching for methods or treatments to control or eliminate resistant bacteria is not new, but there are limitations to their use in *in vivo* applications, such as selectivity

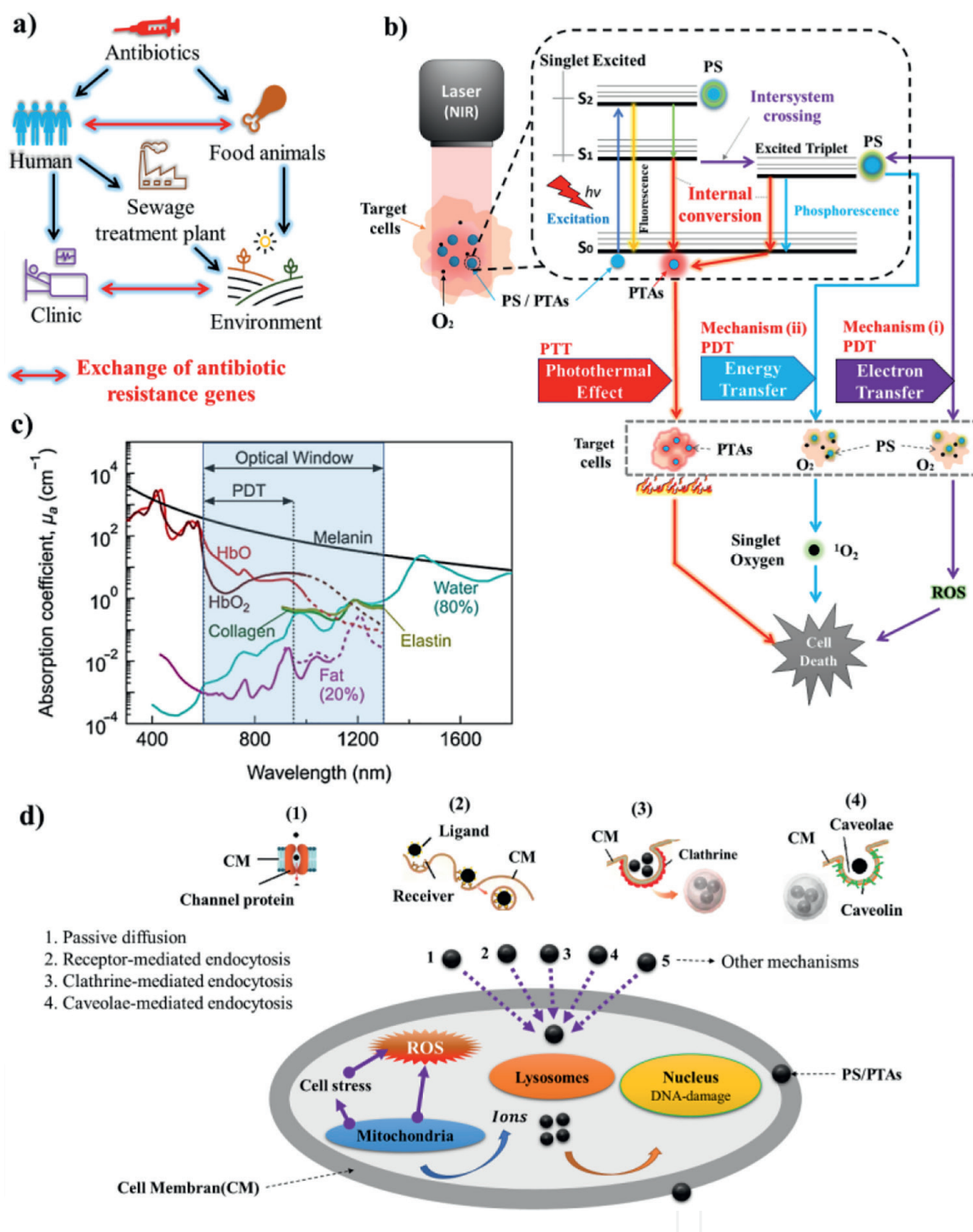


**Figure 1.** (a) Exchange cycle of the genetic mutation of bacteria. (b) ROS and photothermal effect generation mechanisms for cell death in PDT and PTT. (c) Optical window of melamine, water, hemoglobin, and collagen, depending on the absorption coefficient [13]. Copyright 2022 MDPI. (d) Internalization mechanisms of the PS and PTAs in target cells.

and activation control [1]. Nanotechnology has presented successful solutions to this problem, such as metal nanoparticles (NPs) [9], metal oxide nanoparticles [10], carbon-based materials (CBM) [11], and nanocomposites [12], as antibacterial agents. In the CBM group, there are single-walled carbon nanotubes (SWCNTs), multiwalled carbon nanotubes (MWCNTs), graphene (G), graphene oxide (GO), reduced graphene oxide (r-GO), carbon dots (CDs), and fullerenes [4, 6]. These nanotechnology solutions have spread into applications such as water treatment [14–17], antimicrobial

textiles [18], antimicrobial food packaging [19, 20], antibacterial coatings for medical instrumentation and equipment [21], bacterial distinguishment [22], regeneration of living tissues [12, 23], photocatalytic disinfection [1, 3, 12, 24], light-induced acidification [1, 25], photodynamic therapy (PDT) to antibacterial applications or antimicrobial PDT (APDT) [26–29], and photothermal treatment (PTT) or photothermal bacterial lysis (PTBL) [1, 30–33].

On the other hand, thermotherapy is a widely applied technique in medical treatments, mainly in the oncology area [34, 35]. It is based on using heat (conduction, convection, or conversion) to tissues (local, regional, or general) to induce damage to its cellular structure, causing death in target cells [3]. It also promotes an increase in blood flow that facilitates the supply of proteins, nutrients, and oxygen at the injury site. The rise of 1°C in the tissue temperature induces improvement between 10 and 15% of the local tissue metabolism [36]. Thermotherapy comprises two categories, that is, hyperthermia and thermal ablation, depending on the range of temperatures in the treatments. Hyperthermia encompasses a temperature range between 41 and 45°C, while thermal ablation encompasses temperatures above 46°C [37–39]. Thermotherapy supplies heat through different energy sources, for example, radio frequency, microwaves, high-intensity ultrasound, light (visible, near-infrared [NIR], and ultraviolet [UV]), and magnetic fields [40], and its name depends on the energy source.

PTT and PDT are antibacterial techniques that are derived from thermotherapy by using a light source (visible, NIR, and UV) to provide heat and reactive oxygen species (ROS) agents, and they differ mainly in the range of temperature and duration of treatment (PTT: > 46°C, 4–6 min; PDT: 41–45°C, 15–60 min) [13, 41], as well as by the mechanisms of action. PPT is based on the use of photothermal agents (PTAs) that produce heat in the presence of electromagnetic radiation, causing the rupture of cell membranes, protein denaturation, and irreversible cell destruction [5, 42]. If metal nanoparticles (NPs) or metal oxide NPs are used as PTAs, an effect known as “localized surface plasmonic resonance” (LSPR) [43] is produced, which allows the temperature of the nanoparticles to increase. When using CBM as PTAs, heating mechanisms are achieved through nonradiative relaxation pathways (internal conversion) (see **Figure 1b**). For this reason, CBM with high absorption and low fluorescence quantum yield will present higher photothermal conversion efficiency [44].

Antibacterial PDT employs three critical components for its application: photosensitizers (PSs), electromagnetic radiation (typically NIR region), and molecular oxygen ( $O_2$ ). The PS absorbs light and donates electrons or energy interchange with surrounding  $O_2$ , promoting the formation of ROS, inducing irreversible damage to the cell membrane leading to the cell apoptosis or necrosis of the target cell [37]. Two different mechanisms achieve ROS generation as an agent of action in PDT. The first type of ROS is formed by the transfer of electrons between the PS and  $O_2$  or substrate, generating oxygen radicals such as superoxide anion ( $O^{\cdot -}$ ), hydroxyl radical ( $HO^{\cdot}$ ), and hydroperoxyl radical ( $HOO^{\cdot}$ ). This is done by transitioning PS molecules from a ground state ( $S_0$ ) to a singlet excited state ( $S_{1,2}$ ) and the excited triplet state, as shown in **Figure 1b**. In excited triplet states, these PS molecules exchange electrons with a target cell ( $O_2$  mainly), producing free radicals that cause oxidative stress and cell death. The second type of mechanism to generate ROS consists of energy transfer between the PS in an excited triplet state and  $O_2$ , giving rise to singlet oxygen ( $^1O_2$ ), which is more reactive and interacts more with proteins, lipids, and nucleic acids of target cells, in a perimeter of around 20 nm, producing cell apoptosis or necrosis [45, 46].

PPT and PDT are typically used under near-infrared (NIR, 700–950 nm) laser irradiation due to the optical window that this region presents (see **Figure 1c**), in

which absorption by hemoglobin (HbO), melanin, and water is reduced, increasing in this way the availability of photons to interact with the PS or PTAs and greater penetration in tissues [13, 42, 47–49]. The treatment effectiveness improves under an incubation time when the PS and PTAs are internalized into the cells by different mechanisms [45] (see **Figure 1d**). The selectivity of this treatment can improve by tuning the PS and PTAs with agents related to the target cells to be treated [41, 50]. Several CBMs, such as CDs, SWCNTs, and MWCNTs, have been used in PDT and PTT applications as PS and PTAs due to their low toxicity, biocompatibility, tunable fluorescence properties, easy functionalization, and antimicrobial activity, which are ideal for *in vivo* applications [5, 7].

## 2. Graphene oxide and reduced-graphene oxide

Graphene, which is also called the “wonder material,” constitutes a revolutionary discovery of the twenty-first century. This CBM has a two-dimensional planar structure like sheets of  $sp^2$ -hybridized carbon atoms packed into a hexagonal arrangement [48]. Graphene comprises isolated layers of graphite. Graphene possesses unique and fascinating properties such as large surface area, resistance, impermeability, hardness, lightweight, flexibility, and conductivity, which have encouraged its application in diverse and multidisciplinary fields [49]. Therefore, graphene has been employed in medicine, electronics, aerospace, energy, nanotechnology, and so on [50].

Graphene has been used in anticancer therapy, drug delivery, tissue engineering, and biomedical imaging. Nevertheless, pristine graphene is hydrophobic and relatively expensive to prepare. Thus, two alternatives of graphene derivatives have been proposed due to their better water affinity and the ability for mass production: graphene oxide (GO) and reduced-graphene oxide (r-GO) [51, 52]. GO is obtained by an oxidation procedure of graphite [53], generally carrying out the following routes of synthesis: Brodie method, Staudenmaier method, Tour method, Hofmann method, and Hummers method and its modification [54, 55]. On the other hand, r-GO is prepared by a reduction process of GO, commonly by chemical or thermal procedures [56]. The presence of carbon and oxygen functional groups, such as alkoxy, carboxylic, epoxy, hydroxyl, and carbonyl in the basal planes, and peripheries of these graphene derivatives, promotes a better hydrophilic character and solubility than graphene (see **Figure 2a**) and facilitates biointeractions with molecules like nucleic acids and proteins [58, 59]. Furthermore, these linked molecules determine the oxidative level of GO or r-GO [57, 60].

Regarding the antibacterial action of GO and r-GO, referring to the inhibition of growth and microorganism destruction, it is not only attributed to the photoinduced mechanisms like PDT by the generation of ROS or PTT by the generation of heat, but it is also a consequence of their two-dimensional structures. These CBMs physically kill the bacteria by direct contact with the sharp edge layers (thicknesses of 0.8–1.2 Å) of GO or r-GO and scrape the membrane, causing the rupture of the intracellular matrix and, consequently, the microbe's death [52]. The lateral size of GO and r-GO sheets influences the antibacterial effect. It covers the bacterial pathogen due to the electrostatic interaction between the functional groups of GO, r-GO (basal plane), and the bacterial membrane, thus inhibiting their nutrient absorption and proliferation mechanisms, leading to the death of the bacteria. **Figure 2b** shows AFM images of *S. Aureus* and *Escherichia coli* bacteria free of GO and with GO, showing that GO sheets superficially cover (folds formation) the bacteria; monolayer GO sheets

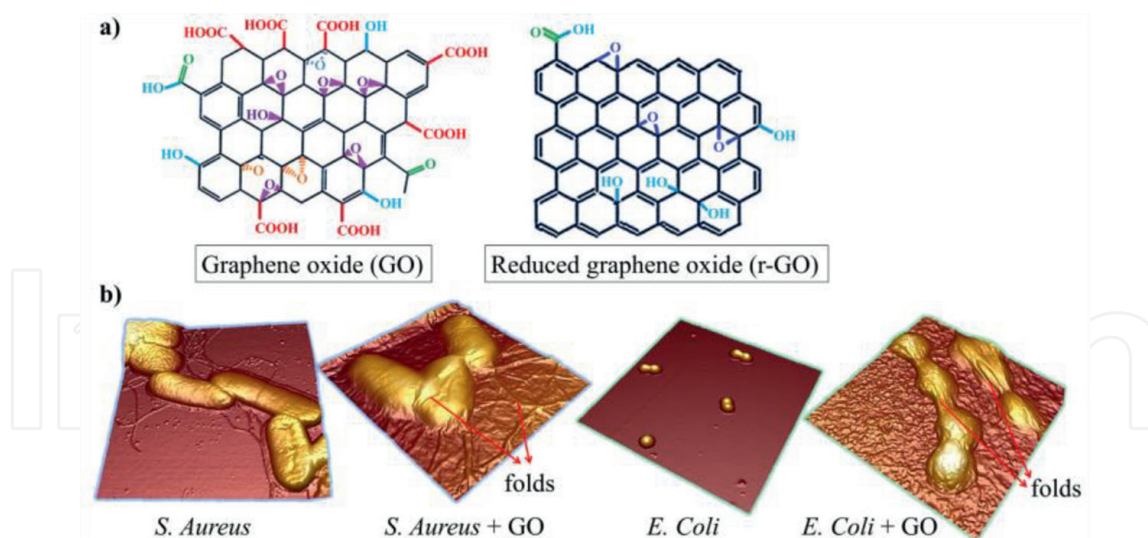


**Figure 2.** (a) Structure of GO and r-GO. Adapted with permission [57]. Copyright 2019 Dove Medical. (b) Atomic force microscopy (AFM) images of *S. aureus* and *E. coli* with and without GO treatment [31]. Copyright 2020 Frontiers.

with an area  $> 0.4 \mu\text{m}^2$  have higher antibacterial activity than GO sheets with an area  $< 0.2 \mu\text{m}^2$  (nanographene oxide [NGO]) [61]. It is important to note that GO and r-GO have intrinsic antibacterial properties; additionally, they attack bacteria by two extra mechanisms: oxidative stress and cell entrapment [62].

## 2.1 Graphene oxide and reduced-graphene oxide in APDT

The antibacterial capacity of GO has been successfully tested against *S. aureus*, *E. coli*, *Klebsiella pneumoniae*, *Pseudomonas aeruginosa*, *Streptococcus mutans*, *Porphyromonas gingivalis*, *Fusobacterium nucleatum*, and *Pseudomonas putida*, among others [63]. It has been demonstrated that GO only produces singlet oxygen ( $^1\text{O}_2$ , energy transfer) under irradiation [64]; hence, it marginally contributes to the biocide capacity compared to the simultaneous generation of electron-hole pairs. In this context, GO with a lateral size of a few micrometers and a thickness of 1 nm reduced the percentage of bacterial survival to  $\sim 24.9\%$  in *E. Coli* under irradiation-simulated sunlight exposure at  $380 \text{ mW}\cdot\text{cm}^{-2}$ , causing bacterial death mainly by the generation of  $^1\text{O}_2$ , to a lesser extent by ROS and intrinsic mechanisms of GO, but with a negligible photothermal effect [65]. The light exposure might reduce GO into r-GO (primarily by electron transfer), forming carbon-centered free radicals, which increase its antibacterial activity. Thus, r-GO performs better as a biocide than GO [63]. Within light-stimulated processes, GO and r-GO are considered ideal materials for the diagnosis and treatment by PDT and PTT because they can be absorbed in the first (650–950 nm) and second (1000–1350 nm) biological windows, where a sufficient tissue penetration of light is attained [31].

To improve the antibacterial capacity of these graphene derivatives, some researchers have proposed its usage along conventional PSs, such as indocyanine green, methylene blue, and toluidine blue [66]. Thus, several works have proved that these composites promoted higher ROS production and an enhanced antibacterial effect compared with the single components. For example, one work used a GO-based composite with indocyanine green to combat *Enterococcus faecalis* (an anaerobic

gram-positive coccus bacterium). It demonstrated that GO upgraded the photodynamic action of indocyanine green, being 1.3 times more effective in the antibiofilm activity [67]. Likewise, nanoparticles of metals such as Ag have been employed to prepare composites showing excellent results in bacteria elimination [68, 69]. One work used GO along Ag nanoparticles (AgNPs) within *in vivo* subcutaneous tests and proved that after 20 min of irradiation with visible light (600 nm), an antibacterial efficacy of 96 and 99% for *E. coli* and *S. aureus* is obtained, respectively [70].

The NGO (~ 21.3 nm) functionalized with DNA-aptamer (short sequences of artificial DNA) is selective with *P. gingivalis*, reducing their viability in the order of 4.33 Log<sub>10</sub> CFU under 980-nm irradiation (1 W for 1 min) and concentration of 1/2 MIC (minimum bacteriostatic concentration, 62.5 nM—obtained without irradiation), as seen in **Figure 3a**. The DNA-aptamer-NGO presents an intrinsic antibacterial activity and increases under irradiation. Their action mechanism reduces bacterial metabolic activity, as observed in **Figure 3b**, which leads to a higher rate of bacterial apoptosis as a function of concentration and irradiation (see **Figure 3c**) [71]. In APDT with GO, there is a dependence between the light dose and the loss of bacterial viability, for example, for the bacteria *E. coli*, its loss of viability is aggravated for 40–60 J·cm<sup>-2</sup> at higher concentrations. However, a higher light dose is required for lower concentration, which also suggests the dependence on GO concentration (see **Figure 3d**). This behavior is similar in *S. aureus* with GO and NGO. That is, there is a threshold of light dose and concentrations of the PS, where the photons are available to excite GO and generate <sup>1</sup>O<sub>2</sub> and the ROS is optimal for causing bacterial death and avoiding affecting healthy tissues.

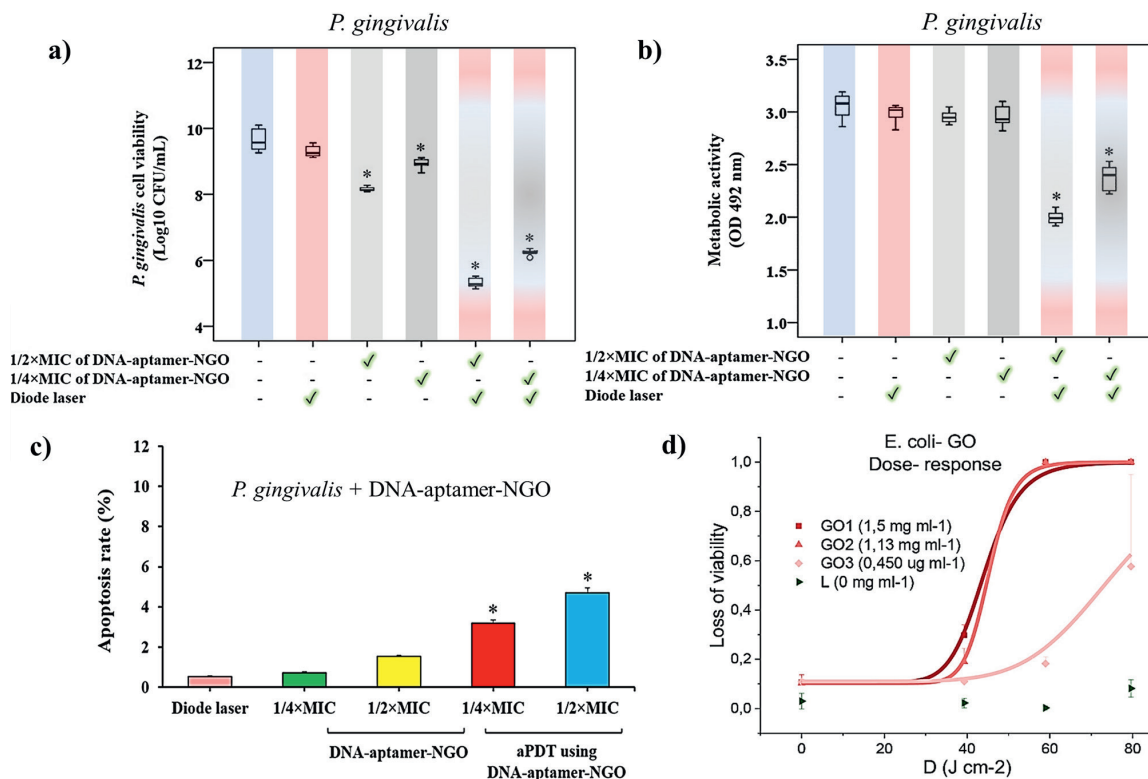


**Figure 3.** (a) Bacterial viability of *P. gingivalis* with DNA-aptamer-NGO in APDT [71]. (b) Metabolic activity of *P. gingivalis* with DNA-aptamer-NGO in APDT [71]. (c) The apoptosis rate of *P. gingivalis* with DNA-aptamer-NGO in APDT [71]. Copyright 2022 Springer Nature. (d) Loss of viability in *E. coli* in APDT with GO as a function of light dose at 630 nm [31]. Copyright 2020 Frontiers.



## 2.2 Graphene oxide and reduced-graphene oxide in antibacterial PTT

The photothermal effect of GO and NGO in antibacterial PTT is a function of its concentration and size. In NGO, its smaller lateral size allows it to keep its temperature below 60°C (in aqueous solutions). In contrast, the temperature of GO having larger lateral size reaches above 60°C under the same conditions (630 nm, 65.5 mW·cm<sup>-2</sup>). Likewise, the heating efficiency is higher in GO (~1.45) than in NGO (~1.3) for a light dose of 60 J·cm<sup>-2</sup> (see **Figure 4a**) [31]. This suggests that a larger surface has greater availability of photons for internal conversion. Therefore, GO and NGO are potential PTAs in antibacterial PTT. However, its selectivity can be improved by incorporating functionalizing agents that positively charge GO for better attraction to bacteria. The amino groups (NH<sub>2</sub>) and polyethylene glycol (PEG) provide a positive charge to GO. Likewise, they can soften the sharp edges of GO, improving its cytotoxicity and biocompatibility but reducing its antimicrobial activity. Even so, nanocomposites, such as GO-PEG-NH<sub>2</sub>, exhibit excellent antibacterial activity in PTT, as seen in **Figure 4b**. These GO nanocomposites inhibit susceptible bacteria such as *E. coli* and *S. aureus* at 50 µm·mL<sup>-1</sup> under 808-nm irradiation and 1.5 W·cm<sup>-2</sup> for 5 min. These nanocomposites partially damage the membrane in the two bacterial strains due to their intrinsic antimicrobial activity. When irradiated, the destruction of the bacterial membrane and a subsequent union of the sample bacteria are produced, as indicated in **Figure 4c** [72].

Furthermore, synergistic mechanisms have been achieved since GO and r-GO also present photothermal effects. One work used amino-functionalized GO and determined that it was easily targeted by electrostatic attraction into gram-negative and gram-positive bacteria surfaces. After the irradiation of 159 mW cm<sup>-2</sup>, it was

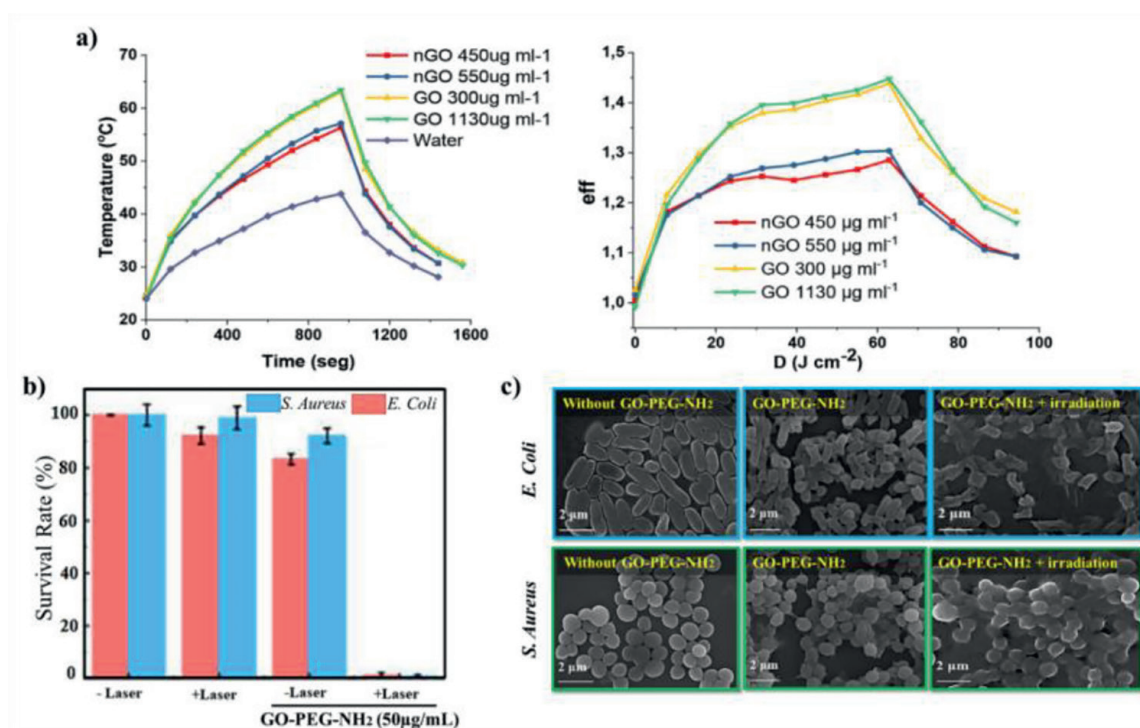


**Figure 4.** (a) Thermal study of NGO and GO in aqueous solution for different irradiation times and concentrations [31]. Copyright 2020 Frontiers. (b) Bacterial survival rate of *S. aureus* and *E. coli* in antibacterial PTT using GO-PEG-NH<sub>2</sub> as PTAs [72]. (c) SEM images of the damage produced by GO-PEG-NH<sub>2</sub> in *E. coli* and *S. aureus* bacteria in antibacterial PTT [72]. Copyright 2020 MDPI.

proved that the temperature increased to 80°C using a concentration of 0.25 mg mL<sup>-1</sup> [73]. Using GO and r-GO as PTAs and PS promises improved antimicrobial activity because bacteria are killed by oxidative stress (APDT) and photothermal effect (PTT), producing synergy between both therapies [74].

### 3. Carbon dots

Carbon dots (CDs) are considered nanospheres of diameter between 1 and 10 nm [54, 56] with carbonaceous nuclei that present sp<sup>2</sup> and sp<sup>3</sup> domains in crystalline and amorphous structures [52, 60, 75]. CDs are divided into the following four groups: carbon quantum dots (CQDs), graphene quantum dots (GQDs), carbon nanodots (CNDs), and carbon polymer dots (CPDs) (CQDs and GQDs exhibit quantum confinement) [60, 61, 65]. The electrons (lone pairs) of sp<sup>2</sup> domains absorb light (visible, NIR, and UV) [1, 57], passing from one energy level ( $\pi$ ) to a higher one  $\pi \rightarrow \pi^*$ , surpassing the forbidden band. Likewise, the presence of functional groups in its structure (typically: -COOH, -OH, and -NH<sub>2</sub>) [76–78] allow surface trap states ( $n$ ) that reduce the bandgap, allowing electrons to absorb light, to reach a higher energy level  $n \rightarrow \pi^*$ . In this way, the CDs generate photoluminescence (PL) by different mechanisms: a photon emission due to the  $\pi$ -conjugated domains of the nucleus (CQDs and GQDs) and photon emission by their surface trap states and by the state of the molecule [76]. In recent years, CDs have gained significant attention for antibacterial applications [76] due to excellent photoluminescence properties, low toxicity, ease of surface functionalization, chemical stability, dispersion in aqueous media, and low cost [23, 61]. Studies of the antimicrobial activity with *S. aureus* and *E. coli* show that CDs have more permeability toward the bacterial cell membrane than traditional antibiotics [4, 62] due to their nanometric size, and it can be improved by reducing the size of CDs [79, 80]. As shown in **Figure 5a**, more significant numbers of small CDs cross the cell membrane than the larger ones.

A highlighting factor of antimicrobial activity is the surface charge of CDs. It must be positive to generate electrostatic attraction between CDs and teichoic and lipoteichoic acids in the gram-positive bacteria cell membrane, likewise with lipopolysaccharides (LPS) in the gram-negative bacteria cell membrane [81]. The surface charge of CDs is modified by their functionalization with suitable molecules, antibiotics, such as biguanide [80], levofloxacin [47], lysine, and folic acid [82], or antimicrobial nanoagents such as AgNPs [83], which increase the antibacterial activity. CDs (4.5–7 nm in size) passivated with amino, carbonyl, and hydroxyl functional groups can diffuse through the *S. aureus* and *E. coli* bacterial membranes without affecting them and continue until CDs disrupt the double helix of naked bacterial DNA, inhibiting bacterial proliferation [81] or activation of other bacteria-killing mechanism observed in **Figure 5b**. If CDs are functionalized with antibiotics, such as levofloxacin hydrochloride (which inhibits bacterial topoisomerase IV and DNA gyrase), the mechanisms to kill bacteria become more potent than the antibiotic action alone [84–86]. In such a way, the CDs induce ROS generation to damage the bacterial cell membrane partially, and the internalization of levofloxacin hydrochloride is easier, causing cytoplasmic leakage and early death of bacteria [47]. A superior feature of CDs is the low probability of causing bacterial resistance due to their excellent biodegradation (short time for resistant response, no efflux pump) [4, 65], and no known enzyme is capable of inhibiting the ROS as HO<sup>•</sup> and <sup>1</sup>O<sub>2</sub> [5].

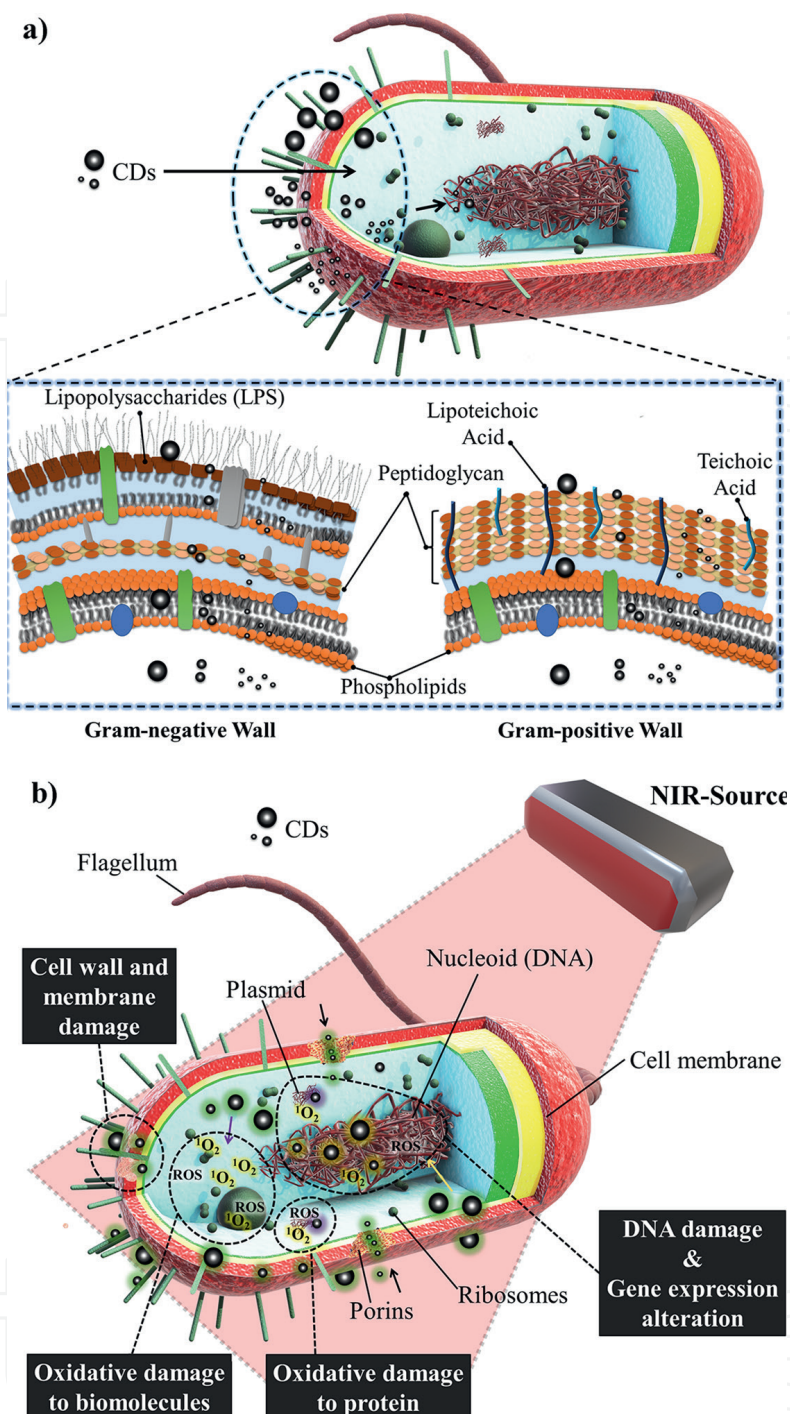


**Figure 5.** (a) Diffusion of CDs of various sizes in the bacterial wall until reaching the DNA. (b) Mechanisms of bacterial death by generating ROS in the presence of CDs.

### 3.1 Carbon dots in APDT

The features of CDs follow the requirements of the new generation of PSs in APDT. CDs achieve inhibition of even MR bacteria such as multidrug-resistant *S. aureus* (MRSA) or multidrug-resistant *Acinetobacter baumannii* (MRAB) at relatively low concentrations ( $32\text{--}64\ \mu\text{g}\cdot\text{mL}^{-1}$ ) of CDs ( $\sim 3\ \text{nm}$ , obtained from 2,4-dihydroxybenzoic acid and 6-bromo-2-naphthol by the solvothermal method), irradiated with red light ( $590\ \text{nm}$ ) by a  $30\text{-mW}\cdot\text{cm}^{-2}$  source for 15 min [87, 88]. Likewise, susceptible bacteria, such as *E. coli*, are inhibited at  $50\ \mu\text{g}\cdot\text{mL}^{-1}$  of Cl-GQDs ( $\sim 3\text{--}5\ \text{nm}$ , obtained from

sucralose by the electrochemical method), irradiated with sunlight simulated in a  $100\text{-mW}\cdot\text{cm}^{-2}$  source for 2 hours [89]. However, the negligible cytotoxicity of these PSs makes them even more attractive for *in vivo* applications. The surface charge of CDs is a significant aspect of CDs-bacterial membrane coupling and must guarantee a positive charge. This surface charge depends on the treatment conditions, for example, pH and dispersion medium; *in vitro* or *in vivo* applications modify surface estate. Usually, the surface charge of CDs gives the Z potential [89]. The surface charge is related to the number of functional groups in CDs as PL emissive centers. With a negative or low charge, the antimicrobial activity decreases due to the low or null electrostatic attraction of the CDs-bacterial membrane and the few surface heteroatoms that promote the formation of ROS [5]. The irradiation times, environmental conditions, irradiation source, and estimation of the light dose administered are crucial in the correct development of APDT. However, in various studies, the incubation time is not reported [64, 77, 78, 90–93]. The incubation time refers to the process of internalization or endocytosis of CDs toward the membrane bacteria (see **Figure 1d**). In this sense, Liu

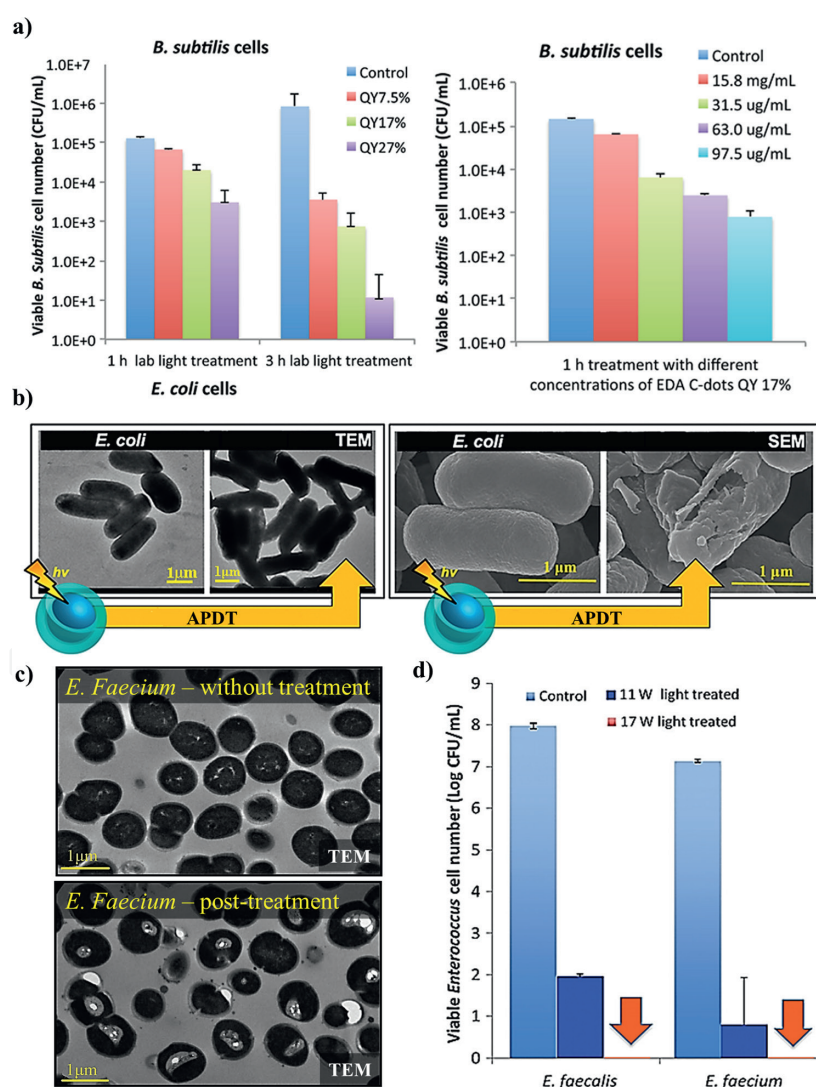


**Figure 6.** (a) Cell viability by CFU number in *Bacillus subtilis* cells for samples with different concentrations and quantum yield (QY) of PL [94]. Copyright 2017 Royal Society of Chemistry. (b) SEM and TEM images of *E. coli* bacteria before and after APDT [5]. Copyright 2020 MDPI. (c) TEM image of *E. faecium* before and after APDT [95]. (d) Inhibition (orange arrows) of *E. faecalis* bacteria by increasing the irradiation dose in APDT [95]. Copyright 2020 Royal Society of Chemistry.

et al. [87] extended the antimicrobial activity of red carbon dots (R-CDs) against MRAB and MRSA by increasing the incubation time from 0 to 45 min, achieving bacterial survival rates of 97.7% at 0 min and 3.3% in MRAB and 7.5% in MRSA at 45 min, because CDs can effectively induce the formation of ROS once inside the bacteria.

An exciting aspect of CDs as PSs in APDT is the dependence between the antibacterial activity and its QY; **Figure 6a** shows this effect. The QY refers to the transformation of absorbed and emitted photons in the structure of the CDs. However, it is common to use the quinine sulfate standard that provides adequate information for the interchange of results [96]. **Figure 6a** indicates a relationship between the irradiation time (hours) and the bacterial viability (CFU mL<sup>-1</sup>) in APDT, as well as a dependence between the bacterial activity (CFU mL<sup>-1</sup>) and the concentration of CDs (μg·mL<sup>-1</sup>) in the treatment. Bacterial viability reduces as more CDs have free electron pairs that promote  $\pi \rightarrow \pi^*$  or  $n \rightarrow \pi^*$  transitions, which, in turn, induce more ROS, thus evidencing the ROS production mechanisms shown in **Figure 1a**, which is the characteristic of APDT. The doping and functionalization of CDs is an essential aspect of QY and significantly affects the antimicrobial activity in APDT and can induce new bacterial death mechanisms, as is the case of bromine-doped carbon nanodots (Br-CNDs). The Br-CNDs in a change of pH (basic-acid-basic) and darkness conditions induce reactive nitrogen species that generate dark toxicity [97].

SEM/TEM observations are a helpful tool to elucidate bacterial damage and are typically acquired before and after APDT. Together with staining assays and confocal laser scanning microscopy imaging techniques, it is possible to propose mechanisms of cell death [23]. **Figure 6b** shows the damage caused to the *E. coli* bacterial membrane before and after APDT. A change in morphology is evidenced by TEM and bacterial lysis by SEM. Similarly, TEM images in **Figure 6c** reveal damage caused to the cytosol of *Enterococcus faecium* bacteria without affecting the cell membrane after APDT [89]. The dose of light used in APDT is a parameter of significant consideration. **Figure 6d** shows that by increasing the power of the irradiation source (0, 11, and 17 W) in APDT, the antibacterial effect increases until viability is inhibited by the *E. faecium* bacteria [89].

### 3.2 Carbon dots in antibacterial PTT

In antibacterial PTT, the CDs cause initial damage to the bacterial membrane due to the absorption of photons and their internal conversion that increases their temperature, as indicated in **Figure 1b** and **5b**. CDs bind to the bacterial membrane mainly by electrostatic interactions and transfer heat to bacteria [98]. In this way, the bacterium becomes vulnerable to heat and allows the incoming of CDs that increase cell damage by inducing the ROS. Therefore, it is common for PTT to synergize with APDT to improve the bacteria-killing mechanism. The initial damage caused by the CDs is increased by incorporating an antibiotic or antibacterial agent, such as quaternary ammonium, which increases the damage to the bacterial membrane, allowing a more significant action than the action of the CDs alone [99]. The photothermal effect is effective in gram-positive and gram-negative bacteria due to the heat the CDs provide, affecting their different structures of peptidoglycan, phospholipids, and LPS. Therefore, CDs in antibacterial PTT present properties like those of broad-spectrum antibiotics. However, the antibacterial effect without irradiation may reduce effectiveness in gram-positive bacteria due to multiple layers of peptidoglycan. It is proved using nanohybrids of GQDs-AgNPs at a concentration of 2 μg·mL<sup>-1</sup> and bacterial strains of *S. aureus* (gram-positive) and *E. coli* (gram-negative). Nevertheless, the

total inhibition of bacterial strains is achieved by irradiation with red light (808 nm) from a  $2\text{-W}\cdot\text{cm}^{-2}$  source for 10 min and the same concentration of GQDs-AgNPs [83].

A relevant aspect of antibacterial PTT is the photothermal performance of CDs (conversion of photons into heat). In dispersion in a liquid medium, they act as heat-emitting sources, and depending on the medium to distribute this thermal energy efficiently, it is possible to reach high temperatures that cause damage to healthy tissue. The temperature reached in *in vivo* and *in vitro* applications is a function of photothermal performance, the concentration of CDs, irradiation time, the dispersion medium, and the dose of light supplied. **Figure 7a** shows the temperature dependence on the dispersion of CDs (doped with Fe), concentration, and irradiation time. The main parameter for temperature control is the concentration of CDs. However, in *in vivo* applications, temperature measurements are usually real time to avoid unwanted tissue damage. This procedure also depends on the depth of the treated infection [83]. CDs doped with Fe or Ag nanoparticles (AgNPs) can acquire a behavior like an enzyme peroxidase (POD) [83] interacting with  $\text{H}_2\text{O}_2$ , increasing its antimicrobial activity (99.85% inhibition *E. coli*) and promoting healing (see **Figure 7b** and **c**).

Antibacterial PTT with CDs allows bone infection treatment through hybrid nanomaterials such as chitosan (CS)-nanohydroxyapatite (nHA) scaffolds doped with CDs (CS-nHA-CDs). CS-nHA-CD scaffolds help as a base material for the new bone tissue with antibacterial features. These antibacterial scaffolds achieve an inhibition (*in vivo*) of up to 97 and 99% for *E. coli* and *S. aureus* bacteria, respectively, under red light irradiation (808 nm,  $1\text{ W}\cdot\text{cm}^{-2}$ ) for 10 min. Healthy tissues reduce the dose of light reaching antibacterial scaffolds. Therefore, the temperature control and thermal performance of these materials are essential [23].

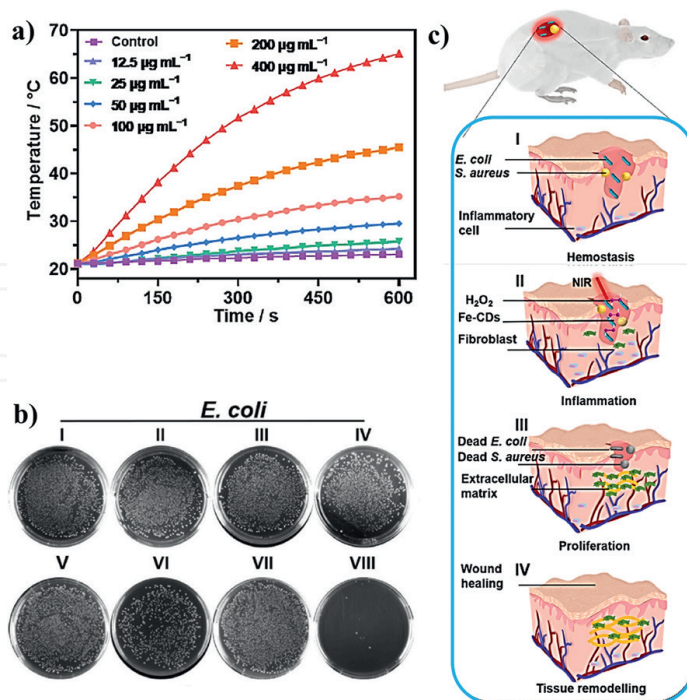


**Figure 7.** (a) Thermal study of CDs doped with Fe for different concentrations as a function of irradiation time. (b) The antibacterial activity of Fe-CDs for a strain of *E. coli*, with an irradiation of  $2\text{ W}\cdot\text{cm}^{-2}$  at 808 nm, (I) control, (II) Fe-CDs, (III)  $\text{H}_2\text{O}_2$ , (IV) Fe-CDs +  $\text{H}_2\text{O}_2$ , (V) NIR, (VI) Fe-CDs + NIR, (VII)  $\text{H}_2\text{O}_2$  + NIR, (VIII) Fe-CDs +  $\text{H}_2\text{O}_2$  + NIR. (c) Scheme of antibacterial PTT in vivo, with wound healing effect. All the images were obtained from [30]. Copyright 2021 Elsevier.

## 4. Carbon nanotubes

CNTs comprise sheets of graphene rolled in the form of a tube, and transverse dimensions are in the nanometric range, but the length is over the nanometric scale. Therefore, CNTs are one-dimensional material. The number of graphene sheets forming CNTs allows the classification of this material into multiwalled carbon nanotubes (MWCNTs) with a diameter of ~10–100 nm and single-wall carbon nanotubes with a diameter of ~0.4–2 nm [100]. CNTs have crystalline  $sp^2$  domains with graphene as a precursor. Their physicochemical structure makes them hydrophobic and cytotoxic. CNTs are usually functionalized with noncovalent bonds to improve their biocompatibility and solubility in aqueous media [6]. The CNTs present a spontaneous interaction with bacteria and a strong absorbance in the NIR. For this reason, CNTs are suitable photothermal antibacterial agents in PTT [1]. CNTs are not eligible for APDT because they energetically reduce or inhibit singlet oxygen  $^1O_2$  generation (SOG) and have QY below ~1 [101]. However, an appropriate functionalization or formation of a nanocomposite can modify their properties, allowing CNTs to perform as PSs. CNTs act like needles in the bacterial cell membrane, inducing damage according to the surface resistance of each bacterial strain. CNTs also act like a nanochannel once located in the bacterial membrane, the needle effect is more evident in SWCNTs due to reduced diameters, and the channel-like effect stands out in MWCNTs [100].

CNTs can be vertically directionally grown, producing a nanoforest of CNTs suitable to inhibit bacterial biofilms, causing immobilization due to their needle-like effect. The nanoforest of CNTs is a nanostructure like insects' wings (biomimetics) with excellent antimicrobial activity by their tower-like nanostructures. **Figure 8a** shows the antibacterial activity of the nanoforest of MWCNTs in a strain of *Klebsiella oxytoca*.

SWCNTs coupled with surfactants in antibacterial PTT show the inhibition of bacterial strains such as *E. coli* and *E. faecium* with more significant antimicrobial activity in *E. faecium*. The *E. faecium* bacterium is more susceptible to surfactants, allowing a better penetration of the CNTs in the cell membrane [103].

### 4.1 Carbon nanotubes in APDT and antibacterial PTT

CNTs' functionalizing agents, such as menthol-zinc phthalocyanine (ZnMintPc), zinc monocarboxyphenoxyphthalocyanine (ZnMCPc), spermine, protoporphyrin IX, or nanocomposites of CNTs with a matrix such as GO and poly (N-vinyl caprolactam-co-poly (ethylene glycol diacrylate)) poly (VCL-co-PEGDA) polymer, significantly improve SOG in antibacterial PDT, generating oxidative damage or alterations in bacterial DNA [12, 27]. The photothermal effect (photons to heat) in MWCNTs is produced by internal conversion, just like GO, because they share the same carbon structure in a hexagonal honeycomb arrangement (see **Figure 8a**). However, magnetic nanoparticles (MNPs) that generate heat by the LSPR effect increase a slightly lower photothermal effect. Thus, MWCNTs (cyan curves) convert photons to heat more efficiently than MNPs (blue curves).

MWCNTs embedded in VCL/PEGDA (hydrogel) and ZnMintPc as PSs form a nanocomposite VCL/PEGDA-MWCNT-ZnMintPc with excellent antibacterial activity (see **Figure 8c**, C1). The complete inhibition of *E. coli* bacteria ascribes to the photothermal effects of MWCNTs (irradiated with a red light at 360 nm in a  $65.5\text{-mW}\cdot\text{cm}^{-2}$  source) and the generation of ROS by the PS (ZnMintPc). The action mechanism of this nanocomposite consists of cell membrane damage by direct contact (see **Figure 8d**) and oxidative damage. The gram-positive bacteria (*S. aureus*) did not completely

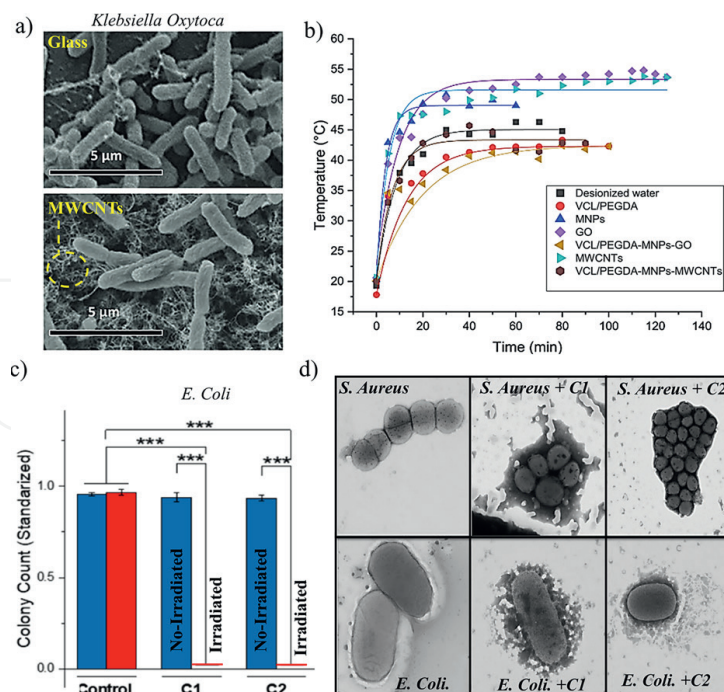


**Figure 8.** (a) SEM observations of morphology and *K. oxytoca* bacteria in a glass substrate and vertical MWCNTs' forest [102]. (b) Evaluation of the photothermal effect of MWCNTs and other molecules of interest as a function of time [12]. (c) Extended plate count method, CFU, of a bacterial strain *E. coli* under NIR irradiation ( $630\text{ nm}$ ,  $65.5\text{ mW}\cdot\text{cm}^{-2}$ ) [12]. Copyright 2016 Royal Society of Chemistry. (d) STEM observations in bacterial strains *S. aureus* and *E. coli* before and after APDT-PTT with different nanocompounds (C1, C2) [12]. Copyright 2022 MDPI.

inhibit. However, the nanocomposite bacteria coupling mechanism is similar. This nanocomposite exhibits synergistic antimicrobial properties in APDT and antibacterial PTT, identical to a nanocomposite with GO and MNPs (C2 in **Figure 8c**) toward *E. coli* bacteria under the same conditions. The potential application of MWCNTs as PTAs and PS (within antibacterial PTT and APDT, respectively), has the advantage that they present an additional mechanism of coupling-bacterial death by its needle-like effect.

## 5. Perspectives

Carbon-based materials (CBMs), such as graphene oxide, reduced-graphene oxide, carbon dots, and carbon nanotubes, have promising possibilities as photosensitizers and photothermal agents within photodynamic and photothermal treatments to combat bacteria. These materials have been used as platforms and components to develop complex composites. Thus, to encourage their practical application in medicine, it is necessary to standardize large-scale production by maintaining high quality, reproducible, and uniform morphology and size of these CBMs.

Besides, exploring their killing or inhibition action against other microorganisms, like viruses and fungi, has become a topic of interest. Hence, it is important to continue the research on the toxicity of these materials in human health and the environment.

Antibacterial photodynamic and photothermal therapies have been extensively investigated in susceptible and multidrug-resistant (MR) monostrain bacteria and MR monostrain biofilms. However, MR dual-strain biofilms can proliferate



synergistically under specific conditions studied in recent years. The wide variety of bacterial pathogens and their potential coupling in biofilms sustained new research to understand and combat this warning to health. In addition, the possibility of continuing to find new multistrain bacteria biofilms acting synergistically in hospital substrates and the obsolete antibiotics proves the seriousness of this bacterial risk. Therefore, it is essential to evaluate, propose, and develop proper culture conditions, as well as the new era of antibacterial agents, including CBMs, for their promising antibacterial activity in thermotherapy treatments.

## 6. Conclusion

This chapter summarizes the recent progress of carbon-based materials (CBMs) as a novel alternative to combat bacteria. The excessive use of antibiotics triggered bacterial resistance that caused severe diseases, even becoming a health risk. Therefore, developing new treatments has become mandatory to overcome this public problem. In this context, several authors have proposed CBMs as antibacterial agents, mainly focusing on their applications within light-assisted treatments as photodynamic and photothermal therapies since they are rapid, affordable, and minimally invasive and have less side effects. The main CBM employed to achieve this aim comprises graphene oxide, reduced-graphene oxide, carbon dots, and carbon nanotubes; nevertheless, the preparation of hybrids and composites has also been proposed to improve their antibacterial effect. Metal nanoparticles, biopolymers, metal oxide nanoparticles, and so on have been employed. We discussed some of the mechanisms whereby bacteria are inhibited or killed. Several works reported in the literature have achieved the complete elimination of bacteria. The most studied species are *E. coli* and *S. aureus*. Hence, this chapter evidences that CBM could be used as a benchmark antimicrobial agent.

## Acknowledgements

The authors would like to thank Escuela Politécnica Nacional.

## Conflict of interest

The authors declare no conflict of interest.

IntechOpen

IntechOpen


### **Author details**

David Giancarlo García Vélez, Karina Janneri Lagos Álvarez  
and María Paulina Romero Obando\*  
Materials Department, National Polytechnic School, Quito, Ecuador

\*Address all correspondence to: [maria.romerom@epn.edu.ec](mailto:maria.romerom@epn.edu.ec)

### **IntechOpen**

---

© 2023 The Author(s). Licensee IntechOpen. This chapter is distributed under the terms of the Creative Commons Attribution License (<http://creativecommons.org/licenses/by/3.0>), which permits unrestricted use, distribution, and reproduction in any medium, provided the original work is properly cited. 

## References

- [1] Feng Y, Liu L, Zhang J, Aslan H, Dong M. Photoactive antimicrobial nanomaterials. *Journal of Materials Chemistry B*. 2017;**5**(44):8631-8652
- [2] Castañeda Gullot C, Ramos SG. Principales pandemias en la historia de la humanidad. *Revista Cubana de Pediatría*. 2020;**92**:1-24
- [3] Kong X, Liu X, Zheng Y, Chu PK, Zhang Y, Wu S. Graphitic carbon nitride-based materials for photocatalytic antibacterial application. *Materials Science and Engineering: R: Reports*. 2021;**145**:100610
- [4] Liang J, Li W, Chen J, Huang X, Liu Y, Zhang X, et al. Antibacterial activity and synergetic mechanism of carbon dots against gram-positive and -negative bacteria. *ACS Applied Bio Materials*. 2021;**4**(9):6937-6945
- [5] Knoblauch R, Geddes CD. Carbon nanodots in photodynamic antimicrobial therapy: A review. *Materials (Basel)*. 2020;**13**(18):2-35
- [6] Paramanantham P, Anju VT, Dyavaiah M, Siddhardha B. Applications of carbon-based nanomaterials for antimicrobial photodynamic therapy. In: Prasad R, editor. *Nanotechnology in the Life Sciences*. Switzerland: Springer, Cham; 2019. pp. 237-259
- [7] Ren Y, Liu H, Liu X, Zheng Y, Li Z, Li C, et al. Photoresponsive materials for antibacterial applications. *Cell Reports Physical Science*. 2020;**1**(11):100245
- [8] Ortez JH, Rankin ID. Manual de pruebas de susceptibilidad antimicrobiana. In: Coyle MB, editor. *Manual de Pruebas de Susceptibilidad Antimicrobiana*. Seattle, Washington: American Society for Microbiology; 2005. p. 242
- [9] Liu Y, Guo Z, Li F, Xiao Y, Zhang Y, Bu T, et al. Multifunctional magnetic copper ferrite nanoparticles as Fenton-like reaction and near-infrared photothermal agents for synergetic antibacterial therapy. *ACS Applied Materials & Interfaces*. 2019;**11**(35):31649-31660
- [10] Al-Karagoly H, Rhyaf A, Naji H, Albukhaty S, Almalki FA, Alyamani AA, et al. Green synthesis, characterization, cytotoxicity, and antimicrobial activity of iron oxide nanoparticles using *Nigella sativa* seed extract. *Green Processing and Synthesis*. 2022;**11**(1):254-265
- [11] Chen S, Saltikov C, Nichols F, Lu JE, Mercado R, Rojas-Andrade MD, et al. Antibacterial activity of Nitrogen-doped Carbon dots enhanced by atomic dispersion of copper. *Langmuir*. 2020;**36**(39):11629-11636
- [12] Cuadrado CF, Díaz-Barrios A, Campaña KO, Romani EC, Quiroz F, Nardecchia S, et al. Broad-spectrum antimicrobial ZnMintPc encapsulated in magnetic-nanocomposites with graphene oxide/MWCNTs based on bimodal action of photodynamic and photothermal effects. *Pharmaceutics*. 2022;**14**(4):2-26
- [13] McGhie BS, Aldrich-Wright JR. Photoactive and luminescent transition metal complexes as anticancer agents: A guiding light in the search for new and improved cancer treatments. *Biomedicines - MDPI*. 2022;**10**:2-4
- [14] El-Gendy NS, Omran BA. Green synthesis of nanoparticles for water treatment. In: Fosso-Kankeu E, editor. *Nano and Bio-Based Technologies for Wastewater Treatment: Prediction and Control Tools for the Dispersion of*

Pollutants in the Environment. Vol. 1.  
2019

[15] Saharan P, Chaudhary GR, Mehta SK, Umar A. Removal of water contaminants by iron oxide nanomaterials. *Journal of Nanoscience and Nanotechnology*. 2014;**14**(1):627-643

[16] Jani M, Arcos-Pareja JA, Ni M. Engineered zero-dimensional Fullerene/Carbon dots-polymer based nanocomposite membranes for wastewater treatment. *Molecules*. 2020;**25**(21):1-28

[17] Israr M, Iqbal J, Arshad A, Aisida SO, Ahmad I. A unique ZnFe<sub>2</sub>O<sub>4</sub>/graphene nanoplatelets nanocomposite for electrochemical energy storage and efficient visible light driven catalysis for the degradation of organic noxious in wastewater. *Journal of Physics and Chemistry of Solids*. 2020;**140**:109333

[18] Doganay D, Kanicioglu A, Coskun S, Akca G, Unalan HE. Silver-nanowire-modified fabrics for wide-spectrum antimicrobial applications. *Journal of Materials Research*. 2019;**34**(4):500-509

[19] Raul PK, Thakuria A, Das B, Devi RR, Tiwari G, Yellappa C, et al. Carbon nanostructures as antibacterials and active food-packaging materials: A review. *ACS Omega*. 2022;**7**:11555-11559

[20] Mousavi SM, Hashemi SA, Kalashgrani MY, Omidifar N, Bahrani S, Rao NV, et al. Bioactive graphene quantum dots based polymer composite for biomedical applications. *Polymers (Basel)*. 2022;**14**(3):2-30

[21] Tonelli AM, Venturini J, Arcaro S, Henn JG, Moura DJ, da Viegas AC, et al. Novel core-shell nanocomposites based on TiO<sub>2</sub>-covered magnetic Co<sub>3</sub>O<sub>4</sub> for biomedical applications. *Journal of Biomedical Materials Research Part B Applied Biomaterials*. 2020;**108**(5):1879-1887

[22] Yang J, Zhang X, Ma YH, Gao G, Chen X, Jia HR, et al. Carbon dot-based platform for simultaneous bacterial distinguishment and antibacterial applications. *ACS Applied Materials & Interfaces*. 2016;**8**(47):32170-32181

[23] Lu Y, Li L, Li M, Lin Z, Wang L, Zhang Y, et al. Zero-dimensional carbon dots enhance bone regeneration, osteosarcoma ablation, and clinical bacterial eradication. *Bioconjugate Chemistry*. 2018;**29**(9):2982-2993

[24] Zhao X, Li J, Liu D, Yang M, Wang W, Zhu S, et al. Self-enhanced carbonized polymer dots for selective visualization of lysosomes and real-time apoptosis monitoring. *iScience*. 2020;**23**(4):100982

[25] Hamblin MR. Antimicrobial photodynamic inactivation: A bright new technique to kill resistant microbes. *Current Opinion in Microbiology* [Internet]. 2016;**33**:67-73 Available from: <https://pubmed.ncbi.nlm.nih.gov/27421070>

[26] Baltazar LM, Ray A, Santos DA, Cisalpino PS, Friedman AJ, Nosanchuk JD. Antimicrobial photodynamic therapy: An effective alternative approach to control fungal infections. *Frontiers in Microbiology*. 2015;**6**:1-11

[27] Qi M, Chi M, Sun X, Xie X, Weir MD, Oates TW, et al. Novel nanomaterial-based antibacterial photodynamic therapies to combat oral bacterial biofilms and infectious diseases. *International Journal of Nanomedicine*. 2019;**14**:6937-6956

[28] Romero MP, Alves F, Stringasci MD, Buzzá HH, Ciol H, Inada NM, et al. One-pot microwave-assisted synthesis of carbon dots and in vivo and in vitro antimicrobial photodynamic applications. *Frontiers in Microbiology*. 2021;**12**:1-13

- [29] Chen Y, Gao Y, Chen Y, Liu L, Mo A, Peng Q. Nanomaterials-based photothermal therapy and its potentials in antibacterial treatment. *Journal of Controlled Release* [Internet]. 2020;**328**:251-262. Available from: DOI: 10.1016/j.jconrel.2020.08.055
- [30] Liu Y, Xu B, Lu M, Li S, Guo J, Chen F, et al. Ultrasmall Fe-doped carbon dots nanozymes for photoenhanced antibacterial therapy and wound healing. *Bioactive Materials*. [Internet]. 2022;**12**:246-256. Available from: DOI: 10.1016/j.bioactmat.2021.10.023
- [31] Romero MP, Marangoni VS, de Faria CG, Leite IS, de Silva CCC e, Maroneze CM, et al. Graphene oxide mediated broad-spectrum antibacterial based on bimodal action of photodynamic and photothermal effects. *Frontiers in Microbiology*. 2020;**10**:1-15
- [32] Cui Q, Yuan H, Bao X, Ma G, Wu M, Xing C. synergistic photodynamic and photothermal antibacterial therapy based on a conjugated polymer nanoparticle-doped hydrogel. *ACS Applied Bio Materials*. 2020;**3**(7):4436-4443
- [33] Yan H, Zhang B, Zhang Y, Su R, Li P, Su W. Fluorescent carbon dot-curcumin nanocomposites for remarkable antibacterial activity with synergistic photodynamic and photothermal abilities. *ACS Applied Bio Materials*. 2021;**4**(9):6703-6718
- [34] Alan JF. *Adaptative Phased Array Thermotherapy for Cancer*. Vol. 2006. Damascus University Publications. United States of America: Artech House; 1999. pp. 1-6
- [35] Kok HP, Cressman ENK, Ceelen W, Brace CL, Ivkov R, Grüll H, et al. Heating technology for malignant tumors: A review. *International Journal of Hyperthermia*. 2020;**37**(1):711-741
- [36] Nadler SF, Weingand K, Kruse RJ. The physiologic basis and clinical applications of cryotherapy and thermotherapy for the pain practitioner. *Pain Physician*. 2004;**7**(3):395-399
- [37] Gabriela NA, Grumezescu AM. Applied sciences photodynamic therapy — An up-to-date review. *Applied Sciences*. 2021;**11**:3626
- [38] Hu T, Wang Z, Shen W, Liang R, Yan D, Wei M. Recent advances in innovative strategies for enhanced cancer photodynamic therapy. *Theranostics*. 2021;**11**(7):3278-3300
- [39] Rhodes LE, De Rie M, Enström Y, Groves R, Morken T, Goulden V, et al. Photodynamic therapy using topical methyl aminolevulinate vs surgery for nodular basal cell carcinoma: results of a multicenter randomized prospective trial. *Archives of Dermatology*. 2004;**140**:17-23
- [40] Estelrich J, Antònia BM. Iron oxide nanoparticles in photothermal therapy. *Molecules*. 2018;**23**(7):2-26
- [41] Pedrosa P, Mendes R, Cabral R, Martins LMDRS, Baptista PV, Fernandes AR. Combination of chemotherapy and Au-nanoparticle phototherapy in the visible light to tackle doxorubicin resistance in cancer cells. *Scientific Reports*. 2018;**8**(1):1-8
- [42] Sun Q, Hou P, Wu S, Yu L, Dong L. The enhanced photocatalytic activity of Ag-Fe<sub>2</sub>O<sub>3</sub>-TiO<sub>2</sub> performed in Z-scheme route associated with localized surface plasmon resonance effect. *Colloids and Surfaces A: Physicochemical and Engineering Aspects*. 2021;**628**:127304
- [43] Hu M, Chen J, Li ZY, Au L, Hartland GV, Li X, et al. Gold nanostructures: Engineering their plasmonic properties for biomedical

applications. *Chemical Society Reviews*. 2006;**35**(11):1084-1094

[44] Xin Q, Shah H, Nawaz A, Xie W, Akram MZ, Batool A, et al. Antibacterial carbon-based nanomaterials. *Advanced Materials*. 2019;**31**(45):1-15

[45] Patil RM, Thorat ND, Shete PB, Bedge PA. Comprehensive cytotoxicity studies of superparamagnetic iron oxide nanoparticles. *Biochemistry and Biophysics Reports*. 2018;**13**:63-72

[46] Lu X, Rycenga M, Skrabalak SE, Wiley B, Xia Y. Chemical synthesis of novel plasmonic nanoparticles. *Annual Review of Physical Chemistry*. 2009;**60**:167-192

[47] Wu LN, Yang YJ, Huang LX, Zhong Y, Chen Y, Gao YR, et al. Levofloxacin-based carbon dots to enhance antibacterial activities and combat antibiotic resistance. *Carbon N Y*. 2022;**186**:452-464

[48] Banerjee AN. Graphene and its derivatives as biomedical materials: Future prospects and challenges. *Interface Focus*. 2018;**8**(3):1-22

[49] Nurunnabi M, Parvez K, Nafiujjaman M, Revuri V, Khan HA, Feng X, et al. Bioapplication of graphene oxide derivatives: Drug/gene delivery, imaging, polymeric modification, toxicology, therapeutics and challenges. *RSC Advances*. 2015;**5**(52):42141-42161

[50] Dhinakaran V, Lavanya M, Vigneswari K, Ravichandran M, Vijayakumar MD. Review on exploration of graphene in diverse applications and its future horizon. *Materials Today Proceedings* [Internet]. 2020;**27**:1-5. DOI: 10.1016/j.matpr.2019.12.369

[51] Hu W, Peng C, Luo W, Lv M, Li X, Li D, et al. Graphene-based antibacterial paper. *ACS Nano*. 2010;**4**(7):4317-4323

[52] Kumar P, Huo P, Zhang R, Liu B. Antibacterial properties of graphene-based nanomaterials. *Nanomaterials*. [Internet]. 2019;**9**(5):737 Available from: <https://www.mdpi.com/2079-4991/9/5/737>

[53] Galván EM, Mateyca C, Ielpi L. Role of interspecies interactions in dual-species biofilms developed in vitro by uropathogens isolated from polymicrobial urinary catheter-associated bacteriuria. *Biofouling*. 2016;**32**(9):1067-1077

[54] Adetayo A, Runsewe D. Synthesis and fabrication of graphene and graphene oxide: A review. *Open Journal of Composite Materials*. 2019;**09**(02):207-229

[55] Yu W, Sisi L, Haiyan Y, Jie L. Progress in the functional modification of graphene/graphene oxide: A review. *RSC Advances*. 2020;**10**(26):15328-15345

[56] Gao W. *Graphene Oxide: Reduction Recipes, Spectroscopy, and Applications* [Internet]. Switzerland: Springer International Publishing; 2015. Available from: <https://books.google.com.ec/books?id=-Z-4CQAAQBAJ>

[57] Bai RG, Muthoosamy K, Manickam S, Hilal-Alnaqbi A. Graphene-based 3D scaffolds in tissue engineering: Fabrication, applications, and future scope in liver tissue engineering. *International Journal of Nanomedicine*. 2019;**14**:5753-5783

[58] Juarez GE, Galván EM. Role of nutrient limitation in the competition between uropathogenic strains of *Klebsiella pneumoniae* and *Escherichia coli* in mixed biofilms. *Biofouling*. 2018;**34**(3):287-298

[59] Verderosa AD, Totsika M, Fairfull-Smith KE. Bacterial biofilm eradication agents: A current review. *Frontiers in Chemistry*. 2019;**7**:1-17

- [60] Harun SW. Handbook of graphene. In: Biomaterials [Internet]. Vol. 7. Malaya: Wiley; 2019. Available from: <https://books.google.com.ec/books?id=ckKdDwAAQBAJ>
- [61] Liu S, Hu M, Zeng TH, Wu R, Jiang R, Wei J, et al. Lateral dimension-dependent antibacterial activity of graphene oxide sheets. *Langmuir*. 2012;**28**(33):12364-12372
- [62] Pulingam T, Thong KL, Appaturi JN, Lai CW, Leo BF. Mechanistic actions and contributing factors affecting the antibacterial property and cytotoxicity of graphene oxide. *Chemosphere*. [Internet]. 2021;**281**:130739. Available from:. DOI: 10.1016/j.chemosphere.2021.130739
- [63] Anand A, Unnikrishnan B, Wei SC, Chou CP, Zhang LZ, Huang CC. Graphene oxide and carbon dots as broad-spectrum antimicrobial agents-a minireview. *Nanoscale Horizons*. 2019;**4**(1):117-137
- [64] Cui L, Ren X, Sun M, Liu H, Xia L. Carbon dots: Synthesis, properties and applications. *Nanomaterials*. 2021;**11**(12):1-38
- [65] Chong Y, Ge C, Fang G, Wu R, Zhang H, Chai Z, et al. Light-enhanced antibacterial activity of graphene oxide, mainly via accelerated electron transfer. *Environmental Science & Technology* [Internet]. 2017;**51**(17):10154-10161. Available from:. DOI: 10.1021/acs.est.7b00663
- [66] Kholikov K, Ilhom S, Sajjad M, Smith ME, Monroe JD, San O, et al. Improved singlet oxygen generation and antimicrobial activity of sulphur-doped graphene quantum dots coupled with methylene blue for photodynamic therapy applications. *Photodiagnosis and Photodynamic Therapy*. 2018;**24**:7-14
- [67] Akbari T, Pourhajibagher M, Hosseini F, Chiniforush N, Gholibegloo E, Khoobi M, et al. The effect of indocyanine green loaded on a novel nano-graphene oxide for high performance of photodynamic therapy against *Enterococcus faecalis*. *Photodiagnosis and Photodynamic Therapy*. [Internet]. 2017;**20**:148-153. DOI: 10.1016/j.pdpdt.2017.08.017
- [68] Ma J, Zhang J, Xiong Z, Yong Y, Zhao XS. Preparation, characterization and antibacterial properties of silver-modified graphene oxide. *Journal of Materials Chemistry* [Internet]. 2011;**21**(10):3350-3352. Available from:. DOI: 10.1039/C0JM02806A
- [69] Xu WP, Zhang LC, Li JP, Lu Y, Li HH, Ma YN, et al. Facile synthesis of silver@ graphene oxide nanocomposites and their enhanced antibacterial properties. *Journal of Materials Chemistry* [Internet]. 2011;**21**(12):4593-4597. Available from:. DOI: 10.1039/C0JM03376F
- [70] Xie X, Mao C, Liu X, Zhang Y, Cui Z, Yang X, et al. Synergistic bacteria killing through photodynamic and physical actions of graphene oxide/Ag/collagen coating. *ACS Applied Materials & Interfaces*. 2017;**9**(31):26417-26428
- [71] Pourhajibagher M, Moghadam SE, Alaeddini M. OPEN DNA - aptamer - nanographene oxide as a targeted bio-theragnostic system in antimicrobial photodynamic therapy against *Porphyromonas gingivalis*. *Scientific Reports*. 2022;**0123456789**:1-18
- [72] Ma G, Qi J, Cui Q, Bao X, Gao D, Xing C. Graphene oxide composite for selective recognition, capturing, photothermal killing of bacteria over mammalian cells. *Polymers (Basel)*. 2020;**12**(5):1-14
- [73] Mei L, Lin C, Cao F, Yang D, Jia X, Hu S, et al. Amino-functionalized

graphene oxide for the capture and photothermal inhibition of bacteria. *ACS Applied Nano Materials*. 2019;2(5):2902-2908

[74] Magro M, Baratella D, Bonaiuto E, de Roger AJ, Vianello F. New perspectives on biomedical applications of iron oxide nanoparticles. *Current Medicinal Chemistry*. 2017;25(4):540-555

[75] Singh V, Joung D, Zhai L, Das S, Khondaker SI, Seal S. Graphene based materials: Past, present and future. *Progress in Materials Science*. [Internet]. 2011;56(8):1178-1271. Available from: DOI: 10.1016/j.pmatsci.2011.03.003

[76] Chung YJ, Kim J, Park CB. Photonic carbon dots as an emerging nanoagent for biomedical and healthcare applications. *ACS Nano*. 2020;14(6):6470-6497

[77] Koutsogiannis P, Thomou E, Stamatis H, Gournis D, Rudolf P. Advances in fluorescent carbon dots for biomedical applications. *Advances in Physics: X*. 2020;5(1):2-37

[78] Das A, Kundelev EV, Vedernikova AA, Cherevkov SA, Danilov DV, Koroleva AV, et al. Revealing the nature of optical activity in carbon dots produced from different chiral precursor molecules. *Light: Science & Applications*. 2022;11(1):1-13

[79] Ran HH, Cheng X, Bao YW, Hua XW, Gao G, Zhang X, et al. Multifunctional quaternized carbon dots with enhanced biofilm penetration and eradication efficiencies. *Journal of Materials Chemistry B*. 2019;7(33):5104-5114

[80] Sun B, Wu F, Zhang Q, Chu X, Wang Z, Huang X, et al. Insight into the effect of particle size distribution differences on the antibacterial activity of carbon dots. *Journal of Colloid and Interface Science*. 2021;584:505-519

[81] Song Y, Lu F, Li H, Wang H, Zhang M, Liu Y, et al. Degradable carbon dots from cigarette smoking with broad-spectrum antimicrobial activities against drug-resistant bacteria. *ACS Applied Bio Materials*. 2018;1(6):1871-1879

[82] Yu M, Zhang G, Li P, Lu H, Tang W, Yang X, et al. Acid-activated ROS generator with folic acid targeting for bacterial biofilm elimination. *Materials Science and Engineering: C*. 2021;127:112225

[83] Chen S, Quan Y, Yu YL, Wang JH. Graphene quantum dot/silver nanoparticle hybrids with oxidase activities for antibacterial application. *ACS Biomaterials Science & Engineering*. 2017;3(3):313-321

[84] Jijie R, Barras A, Bouckaert J, Dumitrascu N, Szunerits S, Boukherroub R. Enhanced antibacterial activity of carbon dots functionalized with ampicillin combined with visible light triggered photodynamic effects. *Colloids Surfaces B Biointerfaces*. 2018;170:347-354

[85] Mezziani MJ, Dong X, Zhu L, Jones LP, Lecroy GE, Yang F, et al. Visible-light-activated bactericidal functions of carbon "quantum" dots. *ACS Applied Materials & Interfaces*. 2016;8(17):10761-10766

[86] Kováčová M, Kleinová A, Vajdák J, Humpolíček P, Kubát P, Bodík M, et al. Photodynamic-active smart biocompatible material for an antibacterial surface coating. *Journal of Photochemistry and Photobiology B: Biology*. 2020;211:112012

[87] Liu W, Gu H, Ran B, Liu W, Sun W, Wang D, et al. Accelerated antibacterial red-carbon dots with photodynamic therapy against multidrug-resistant *Acinetobacter baumannii*. *Science China Materials*. 2022;65(3):845-854



- [88] Xia C, Zhu S, Feng T, Yang M, Yang B. Evolution and synthesis of carbon dots: From carbon dots to carbonized polymer dots. *Advancement of Science*. 2019;**6**(23):2-23
- [89] Wang L, Li Y, Wang Y, Kong W, Lu Q, Liu X, et al. Chlorine-doped graphene quantum dots with enhanced anti- and pro-oxidant properties. *ACS Applied Materials & Interfaces*. 2019;**11**(24):21822-21829
- [90] Khan ZG, Patil PO. A comprehensive review on carbon dots and graphene quantum dots based fluorescent sensor for biothiols. *Microchemical Journal*. 2020;**157**:105011
- [91] Li H, Kang Z, Liu Y, Lee ST. Carbon nanodots: Synthesis, properties and applications. *Journal of Materials Chemistry*. 2012;**22**(46):24230-24253
- [92] Lim SY, Shen W, Gao Z. Carbon quantum dots and their applications. *Chemical Society Reviews*. 2015;**44**(1):362-381
- [93] Sowers KL, Hou Z, Peterson JJ, Swartz B, Pal S, Prezhdo O, et al. Photophysical properties of CdSe/CdS core/shell quantum dots with tunable surface composition. *Chemical Physics*. 2016;**471**:24-31
- [94] Al Awak MM, Wang P, Wang S, Tang Y, Sun YP, Yang L. Correlation of carbon dots' light-activated antimicrobial activities and fluorescence quantum yield. *RSC Advances*. 2017;**7**(48):30177-30184
- [95] Abu Rabe DI, Mohammed OO, Dong X, Patel AK, Overton CM, Tang Y, et al. Carbon dots for highly effective photodynamic inactivation of multidrug-resistant bacteria. *Materials Advances*. 2020;**1**(3):321-325
- [96] Dou Q, Fang X, Jiang S, Chee PL, Lee TC, Loh XJ. Multi-functional fluorescent carbon dots with antibacterial and gene delivery properties. *RSC Advances*. 2015;**5**(58):46817-46822
- [97] Knoblauch R, Harvey A, Ra E, Greenberg KM, Lau J, Hawkins E, et al. Antimicrobial carbon nanodots: Photodynamic inactivation and dark antimicrobial effects on bacteria by brominated carbon nanodots. *Nanoscale*. 2021;**13**(1):85-99
- [98] Qie X, Zan M, Gui P, Chen H, Wang J, Lin K, et al. Design, synthesis, and application of carbon dots with synergistic antibacterial activity. *Frontiers in Bioengineering and Biotechnology*. 2022;**10**:1-9
- [99] Chu X, Zhang P, Wang Y, Sun B, Liu Y, Zhang Q, et al. Near-infrared carbon dot-based platform for bioimaging and photothermal/photodynamic/quaternary ammonium triple synergistic sterilization triggered by single NIR light source. *Carbon N Y*. 2021;**176**:126-138
- [100] Mocan T, Matea CT, Pop T, Mosteanu O, Buzoianu AD, Suciuc S, et al. Carbon nanotubes as anti-bacterial agents. In: *Cellular and Molecular Life Sciences*. Vol. 74. Switzerland: Birkhauser Verlag AG; 2017. pp. 3467-3479
- [101] Albert K, Hsu HY. Carbon-based materials for photo-triggered theranostic applications. *Molecules*. 2016;**21**(11):1-29
- [102] Malek I, Schaber CF, Heinlein T, Schneider JJ, Gorb SN, Schmitz RA. Vertically aligned multi walled carbon nanotubes prevent biofilm formation of medically relevant bacteria. *Journal of Materials Chemistry B*. 2016;**4**(31):5228-5235
- [103] Dong L, Henderson A, Field C. Antimicrobial activity of single-walled carbon nanotubes suspended in different surfactants. *Journal of Nanotechnology*. 2012;**2012**:1-7